Apoptosis (2018) 23:299–313
https://doi.org/10.1007/s10495-018-1455-x

Critical contribution of RIPK1 mediated mitochondrial dysfunction and oxidative stress to compression-induced rat nucleus pulposus cells necroptosis and apoptosis

Songfeng Chen[1] · Xiao Lv[2] · Binwu Hu[2] · Lei Zhao[2] · Shuai Li[2] · Zhiliang Li[2] · Xiangcheng Qing[2] · Hongjian Liu[1] · Jianzhong Xu[1] · Zengwu Shao[2]

Published online: 28 April 2018

Abstract

The aim of this study was to investigate whether RIPK1 mediated mitochondrial dysfunction and oxidative stress contributed to compression-induced nucleus pulposus (NP) cells necroptosis and apoptosis, together with the interplay relationship between necroptosis and apoptosis in vitro. Rat NP cells underwent various periods of 1.0 MPa compression. To determine whether compression affected mitochondrial function, we evaluated the mitochondrial membrane potential, mitochondrial permeability transition pore (mPTP), mitochondrial ultrastructure and ATP content. Oxidative stress-related indicators reactive oxygen species, superoxide dismutase and malondialdehyde were also assessed. To verify the relevance between oxidative stress and necroptosis together with apoptosis, RIPK1 inhibitor necrostatin-1(Nec-1), mPTP inhibitor cyclosporine A (CsA), antioxidants and small interfering RNA technology were utilized. The results established that compression elicited a time-dependent mitochondrial dysfunction and elevated oxidative stress. Nec-1 and CsA restored mitochondrial function and reduced oxidative stress, which corresponded to decreased necroptosis and apoptosis. CsA down-regulated mitochondrial cyclophilin D expression, but had little effects on RIPK1 expression and pRIPK1 activation. Additionally, we found that Nec-1 largely blocked apoptosis; whereas, the apoptosis inhibitor Z-VAD-FMK increased RIPK1 expression and pRIPK1 activation, and coordinated regulation of necroptosis and apoptosis enabled NP cells survival more efficiently. In contrast to Nec-1, SiRIPK1 exacerbated mitochondrial dysfunction and oxidative stress. In summary, RIPK1-mediated mitochondrial dysfunction and oxidative stress play a crucial role in NP cells necroptosis and apoptosis during compression injury. The synergistic regulation of necroptosis and apoptosis may exert more beneficial effects on NP cells survival, and ultimately delaying or even retarding intervertebral disc degeneration.

Keyword Mitochondrial dysfunction · Oxidative stress · Compression · Nucleus pulposus cells · Necroptosis · Apoptosis

Abbreviations

IVD	Intervertebral disc
IVDD	IVD degeneration
NP	Nucleus pulposus
RIPK1	Receptor-interacting protein kinase 1
RIPK3	Receptor-interacting protein kinase 3
MLKL	Mixed lineage kinase domain-like
PCD	Programmed cell death
NF-κB	Nuclear factor-κB
MDA	Malondialdehyde
SOD	Superoxide dismutase
mtROS	Mitochondrial ROS
LDH	Lactate dehydrogenase
CypD	Cyclophilin D
MMP	Mitochondrial membrane potential
mPTP	Mitochondrial permeability transition pore
SiRNA	Small interfering RNA
Nec-1	Necrostatin-1
z-VAD	Z-VAD-FMK

Songfeng Chen, Xiao Lv and Binwu Hu have contributed equally to this work.

✉ Songfeng Chen
csfzdyfygk@163.com

✉ Zengwu Shao
szwpro@163.com

[1] Department of Orthopaedics, The First Affiliated Hospital of Zhengzhou University, Zhengzhou 450052, China

[2] Department of Orthopaedics, Union Hospital, Tongji Medical College, Huazhong University of Science and Technology, Wuhan 430022, China

CsA	Cyclosporine A
NAC	*N*-acetyl-l-cysteine
BHA	Butyl-4-hydroxyanisole
NS	No significant statistical significance

Introduction

Intervertebral disc degeneration (IVDD) is one of the most common orthopedic ailments, leading to disability of afflicted individuals [1, 2]. The intervertebral disc (IVD), a load-bearing component, is subjected to various kinds of mechanical loading, which can be adaptive or pathological depending on the intensity of the load. For example, a moderate mechanical stimulus exerts protective effect on IVD, while excessive mechanical force often exacerbates IVD cells death [3, 4]. The central gelatinous nucleus pulposus (NP) is the key constituent part of IVD and the effects of pathological loading are generally more severe in NP cells than other types of IVD cells in compression-induced disc degeneration [5]. The decline of NP cells number, which is the main feature of IVDD, is closely related to programmed cell death (PCD) [6]. Moreover, in models of compression, NP cells undergo apoptosis and autophagic cell death [7–9]. However, single regulation of apoptosis or autophagy does not provide an effective protective role against NP cells death [7–9].

Necroptosis, known as type III PCD, is a caspase-independent manner of PCD pathway that was originally defined by Degterev et al. first [10]. In the majority of cases, it is largely dependent on activation of receptor-interacting protein kinase 1 (RIPK1), then the activated RIPK1 binds with and activates receptor-interacting protein kinase 3 (RIPK3) to form the necrosome. These events activate mixed lineage kinase domain-like (MLKL), and initiate necroptosis [11, 12]. Recently, we have reported that RIPK1/RIPK3/MLKL axis-mediated necroptosis plays a pivotal role in compression-induced rat NP cells death [13]. This was the first documentation of compression-mediated necroptosis in IVDD, and has opened a novel perspective for the further elucidation of NP cells death mechanism.

Mitochondria, the fundamental organelles for eukaryotic cells, could produce adenosine-triphosphate (ATP) and regulate cell proliferation and death [14]. Emerging evidence reveals that mitochondrial dysfunction, including mitochondrial membrane potential (MMP) depolarization, enhanced mitochondrial permeability transition pore (mPTP) opening, and mitochondrial cristae disruption, is closely involved in necroptosis and apoptosis [15]. In sharp contrast, some other evidence demonstrates that mitochondrial dysfunction may be dispensable in the occurrence of necroptosis and apoptosis [16, 17]. Mitochondria are an important source of free radicals, which can induce oxidative stress, leading to cell death. Within this context, reactive oxygen species (ROS), a predominant indicator of oxidative stress, is a byproduct of mitochondrial respiratory pathway [18]. However, some ROS generation is important for maintenance of redox-dependent signaling as moderate ROS promotes cell survival; whereas, excessive level of ROS induces the damage of macromolecules and organelles, such as DNA and mitochondria, leading to cell damage or even death [19].

Malondialdehyde (MDA), an indicator of lipid peroxidation, can be used to evaluate oxidative damage. In contrast, superoxide dismutase (SOD), is an important antioxidative enzyme and plays an important role in reducing oxidative stress through metabolism of superoxide. Meanwhile, excessive MDA and reduced SOD activity could reflect mitochondrial dysfunction [20, 21]. Similar to the role of mitochondrial dysfunction, the specific role of oxidative stress in compression-mediated necroptosis and apoptosis of NP cells has not been determined. Under certain circumstances, mitochondrial dysfunction and oxidative stress may play critical roles in IVDD process [22]. Hence, the delineation of the molecular mechanism of mitochondrial dysfunction and oxidative stress in regulating NP cells necroptosis and apoptosis is potentially significant.

In the present study, we systematically addressed the definite role of mitochondrial dysfunction and oxidative stress in compression-induced rat NP cells necroptosis and apoptosis. Necroptosis and apoptosis often interact with each other and together determine the final fate of the cells [11, 23]. We also interrogated the interplay between necroptosis and apoptosis to elucidate an efficient strategy to prevent NP cells death.

Materials and methods

Isolation and culture of primary rat NP cells

The protocol was approved by animal experimentation committee of Huazhong University of Science and Technology. The Sprague-Dawley rats (3 months old) were obtained from Experimental Animal Center of Tongji Medical College, Huazhong University of Science and Technology. The extraction and culture method of rat NP cells were performed as previously described [9, 13, 22]. The second generation NP cells were used throughout the experiments.

Compression and pharmacological treatment of rat NP cells

A protocol previously established in our lab was used, in which the NP cells were cultured in stainless steel pressure vessel to mimic in vivo conditions [9, 13, 22, 24]. The apparatus was constructed to withstand up to 1.0 MPa compression [9, 13, 22, 24]. The RIPK1 inhibitor Nec-1

(Sigma, USA), apoptosis inhibitor Z-VAD-FMK (Merck, Germany), the antioxidants NAC, BHA and mPTP inhibitor CsA (Merck, Germany) were applied to experimental groups, while control groups were given the isopyknic DMSO as a vehicle control. The pressure vessel was filled with a small quantity of distilled water to maintain adequate humidity and then placed in an incubator at 37 °C.

Our previous experiments have demonstrated that when exposed to compression, the level of necroptosis in NP cells significantly increased from 12 to 48 h compared to 0 h, and peaked between 24 and 36 h [13]. Meanwhile, with compression exposure time prolonged, the apoptosis level also peaked at 36 h [22]. Thus, 24 and 36 h compression-treated time periods were chosen in this study.

Evaluation of MMP

The MMP of rat NP cells was examined after 24 and 36 h compression as previously described [22, 24]. The cells were probed by fluorescence probe 5,5′,6,6′-tetrachloro-1,1′,3,3′-tetraethyl-benzimidazolylcarbocyanine iodide (JC-1, Beyotime, China) staining according to the manufacturer's instructions. Finally, the NP cells samples were analyzed by flow cytometry (BD LSRII, Becton Dickinson) and observed under laser scan confocal microscope (LSM, Zeiss, Germany).

Measurement of mPTP

The mPTP of rat NP cells was detected by mPTP Fluorescence Assay Kit (Genmed, China) after 24 and 36 h compression according to the manufacturer's instructions as previously described [22]. Finally, the NP cells samples were analyzed by flow cytometry.

Mitochondrial ultrastructure

The mitochondrial ultrastructure of rat NP cells was examined by transmission electron microscope (TEM), which was performed as previously described [9, 13]. The cells were collected after 36 h compression and suspension of the cells was pelleted (15 min at 1000 g) and supernatant was discarded. Cells were fixed with 2.5% glutaraldehyde for 2 h at room temperature. Then cells were postfixed for 2 h with 1% osmium tetroxide, followed by dehydration steps in ethanol, infiltration and embedding in epon 812. Ultimately, the ultrathin sections were stained with uranyl acetate and lead citrate, and examined with Tecnai G2 12 TEM (FEI Company, Holland).

The ATP production assay

The cellular ATP content was measured using ATP Assay Kit (Beyotime, China). The NP cells were incubated in 200 µl of ATP assay lysis buffer. The supernatant was collected by centrifuging at 12,000×*g* for 5 min at 4 °C and quantified using BCA Protein Assay Kit (Beyotime, China). Then, 100 µl ATP detection reagent was added to 100 µl supernatant, and the firefly luciferase activity was detected and analyzed by luminescence spectrometry (EnSpire, USA). The ATP level was normalized to cellular protein concentration and expressed as percentage relative to the control.

Measurement of ROS

After 24 and 36 h compression, the ROS generation of rat NP cells was revealed using 2′-7′-dihydrodichlorofluoroscein diacetate (DCFH-DA, Sigma, USA), which is oxidized into the fluorescent dichlorofluorescein (DCF) when the ROS generation increased. Briefly, after staining with 10 µM DCFH-DA in the dark at 37 °C for 30 min, the mean fluorescence intensity (MFI) was analyzed using flow cytometry.

Mitochondrial ROS (mtROS) analysis

MitoSOX red was used to estimate mitochondrial ROS. MitoSOX red is a live-cell permeant fluorogenic dye for selective detection of superoxide in mitochondria, and it can emit red fluorescence when oxidized by superoxide. After 24 and 36 h compression, the NP cells were incubated with 5 µM MitoSOX red in the dark at 37 °C for 30 min. Then the NP cells were washed twice and suspended in 200 µl PBS, and analyzed by flow cytometry.

Determination of MDA and SOD activity

The MDA content was measured using a Lipid Peroxidation MDA Assay Kit (Beyotime, China) according to the manufacturer's instructions. The cells were lysed in lysis buffer and centrifuged at 1600 g for 15 min. The supernatant was reacted with the thiobarbituric acid (TBA), and then measured using spectrophotometer (Bio-Tek, USA) at 535 nm. The content of MDA was expressed as nmol/mg protein. The SOD activity was measured using a SOD Assay Kit (Beyotime, China). The cells were collected, washed twice with PBS and centrifuged at 4000 rpm for 15 min. The supernatant was collected to determine SOD activity using spectrophotometer according to the instructions. The results were expressed as U/mg protein.

Determination of cell viability

The rat NP cells were seeded in 96-well culture plates at a density of 2×10^3 cells per well. At each time point, the cell viability was measured using cell counting kit-8 (CCK-8, Dojindo, Japan) according to the manufacturer's instructions [9, 13, 22]. The cell viability was assessed through absorbance detection at 450 nm using spectrophotometer (Bio-Tek, USA).

Annexin V-FITC and propidium iodide (PI) positive ratio assay

The apoptotic and necrotic ratio of rat NP cells were determined using Annexin V-FITC Apoptosis Detection Kit (Nanjing Keygen Biotech, China). At each time point, the cells were harvested, stained according to the manufacturer's instructions and then analyzed by flow cytometry and observed under LSM. The methods of Annexin V-FITC and PI double-staining together with PI single-staining allowed us to quantify the apoptotic cells (Annexin V positive) and necrotic cells (PI positive).

Lactate dehydrogenase (LDH) release assay

After 24 and 36 h compression, the release of LDH in culture medium was measured to determine rat NP cells cytotoxicity according to the manufacturer's instructions (Beyotime, China) using the automated chemistry analyzer. LDH release activity was presented as the ratio of LDH in the culture medium to total cellular LDH and fold to the control group.

Western-blot analysis

At each time point, rat NP cells were harvested, and lysed. Protein concentration of the lysate was determined using an enhanced BCA protein assay kit (Beyotime, China). Then the whole lysate was separated using SDS polyacrylamide gel electrophoresis and transferred onto the polyvinylidene fluoride membranes. The membranes were blocked with 5% bovine serum albumin in Tris-buffered saline and Tween 20 (TBST) for 1 h at room temperature and then incubated overnight at 4 °C with primary antibodies against RIPK1 (1:500, CST, USA), phospho-PKA substrate (1:1000, CST, USA), Bcl-2 (1:500, Abcam, USA), Cleaved-Caspase3 (1:500, Abcam, USA), Cleaved-Caspase8 (1:500, Proteintech, China), Cleaved-Caspase9 (1:200, Proteintech, China), Cleaved-PARP (1:500, Proteintech, China), CypD (1:200, Santa Cruz, USA), GAPDH (1:5000, Abcam, UK). The membranes were washed three times and incubated with the respective peroxidase-conjugated secondary antibodies for 2 h. Finally, the protein was developed using the enhanced chemiluminescence (ECL) method according to the manufacturer's instructions.

Quantitative real-time PCR analysis

At each time point, the total RNA of rat NP cells was extracted using Trizol reagent (Invitrogen, USA). The above obtained RNA was transcribed into complementary DNA. The primer sequences used for real-time PCR were as follows: RIPK1: 5′-TCCTCGTTGACCGTGAC-3′,5′-GCCTCCCTCTGC TTGTT-3′; GAPDH: 5′-CGCTAACATCAAATGGGG TG-3′,5′-TTGCTGACAATCTTGAGGGAG-3′. Gene level was quantified using a standard PCR kit and SYBR Green/ Fluorescein qPCR Master Mix (2X) (Fermentas, Canada) on an ABI Prism 7900HT sequence detection system (Applied Biosystems, USA). The gene expression was subjected to analysis of amplification curve, and the data was analyzed using the $2^{-\Delta\Delta CT}$ method and normalized to house-keeping gene GAPDH.

Transfection of small interfering RNA

Rat SiRIPK1 was designed and manufactured by Biomics (Biomics Biotechnologies Co. Ltd, China) according to current guidelines [13]. The NP cells were treated with three independent SiRIPK1, the sequences of each are as follows: 5′-GGAACAACGGAGTATATAAdTdT-3′,5′-UUAUAU GUUGUUCCdTdT-3′; 5′-GUCUUCGCUAACACCACU AdTdT-3′,5′-UAGUGGUGUUAGCGAAGACdTdT-3′;5′-GGATAATCGTGGAGATCATdTdT-3′,5′-AUGAUCUCC ACGAUUAUCCdTdT-3′ respectively. Then the effective target sequence was selected. The NP cells were transfected with effective sequence at a concentration of 100 pmol/10^5 cell using lipofectamine RNAi MAX (invitrogen). 24 h later, the transfected cells were digested and recultivated for subsequent experiments.

Statistical analysis

All data was shown as mean ± standard deviation (SD) from at least three independent replicates. Statistical analysis was performed using the IBM SPSS software package 20.0. Multiple groups were analyzed by one-way analysis of variance (ANOVA), followed by least significant difference (LSD) analysis. Student's-*t* tests were also performed to analyze the differences between the two groups. A probability of $P < 0.05$ was considered as statistical significance.

Results

Nec-1 or CsA ameliorates compression-induced MMP loss and mPTP opening

The normal cells stained with JC-1 exhibit abundant red along with little green fluorescence. The JC-1 aggregates are dispersed to monomeric form (green fluorescence) when the cells undergo some extent damages. Compared with 0 h group, a time-dependent MMP loss was observed, as indicated by the decrease in red and increase in green fluorescence with the extension of compression time, implying that mitochondrial damage occurred (Fig. 1a–c, $P < 0.01$). Meanwhile, 20 μM Nec-1 ameliorated 24 and 36 h compression-induced MMP loss (Fig. 1a–c, $P < 0.01$). Then CsA, which restricts mPTP opening by interacting with cyclophilin D (CypD), an essential structural component of mPTP, was introduced into current study. Similar

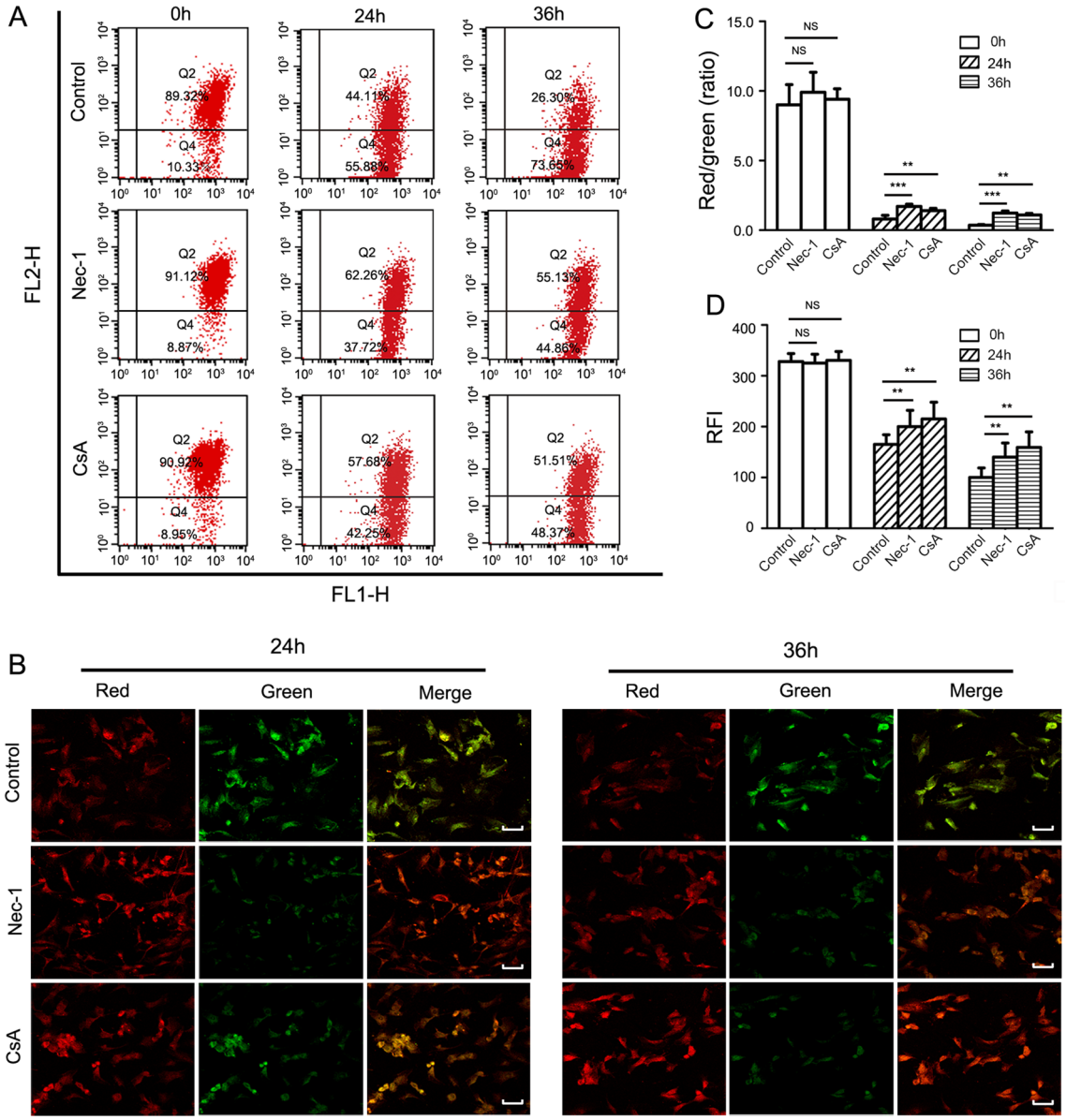

Fig. 1 Nec-1 (20 μM) or CsA (10 μM) inhibits 24 and 36 h compression-induced MMP loss and mPTP opening in rat NP cells. **a** Representative dot plot of MMP in NP cells by flow cytometry after JC-1 staining. **b** Typical fluorescence photomicrograph of MMP loss in NP cells by LSM. **c** The quantitative MMP in NP cells is expressed as the ratio of red over the green fluorescence intensity by flow cytometry. **d** The quantitative relative fluorescence intensity (RFI) of mPTP in NP cells by flow cytometry. Scale bars = 20 μM. Values are expressed as mean ± SD from four independent experiments (n = 4, $^{*}P < 0.05$, $^{**}P < 0.01$, $^{***}P < 0.001$ vs. control)

to Nec-1, 10 μM CsA prevented MMP loss in NP cells at both 24 and 36 h time points (Fig. 1a–c, $P < 0.01$).

A key feature of necroptosis is the enhanced mPTP opening. The value of RFI decreased in a time-dependent manner after 24 and 36 h compression, which implied the enhanced mPTP opening relative to 0 h (Fig. 1d, $P < 0.01$). In presence of Nec-1 or CsA, the 24 and 36 h compression-induced RFI loss were partially attenuated (Fig. 1d, $P < 0.01$). These results supported that Nec-1 and CsA alleviated rat NP cells necroptosis via inhibiting the opening of mPTP.

Nec-1 or CsA restores compression-induced mitochondrial ultrastructure collapse of NP cells

Under baseline, 0 h control condition, mitochondrial structural integrity in NP cells was obvious (Fig. 2a). When compression time was prolonged to 36 h, the mitochondria showed severe damage with swollen, vacuolar and fractured structures (Fig. 2b). When treated with Nec-1 (20 μM) or CsA (10 μM), the mitochondrial morphology displayed varying degrees of recovery, which exhibited few swollen and slightly broken mitochondrial organelles (Fig. 2c, d). These indicated that Nec-1 or CsA protected rat NP cells

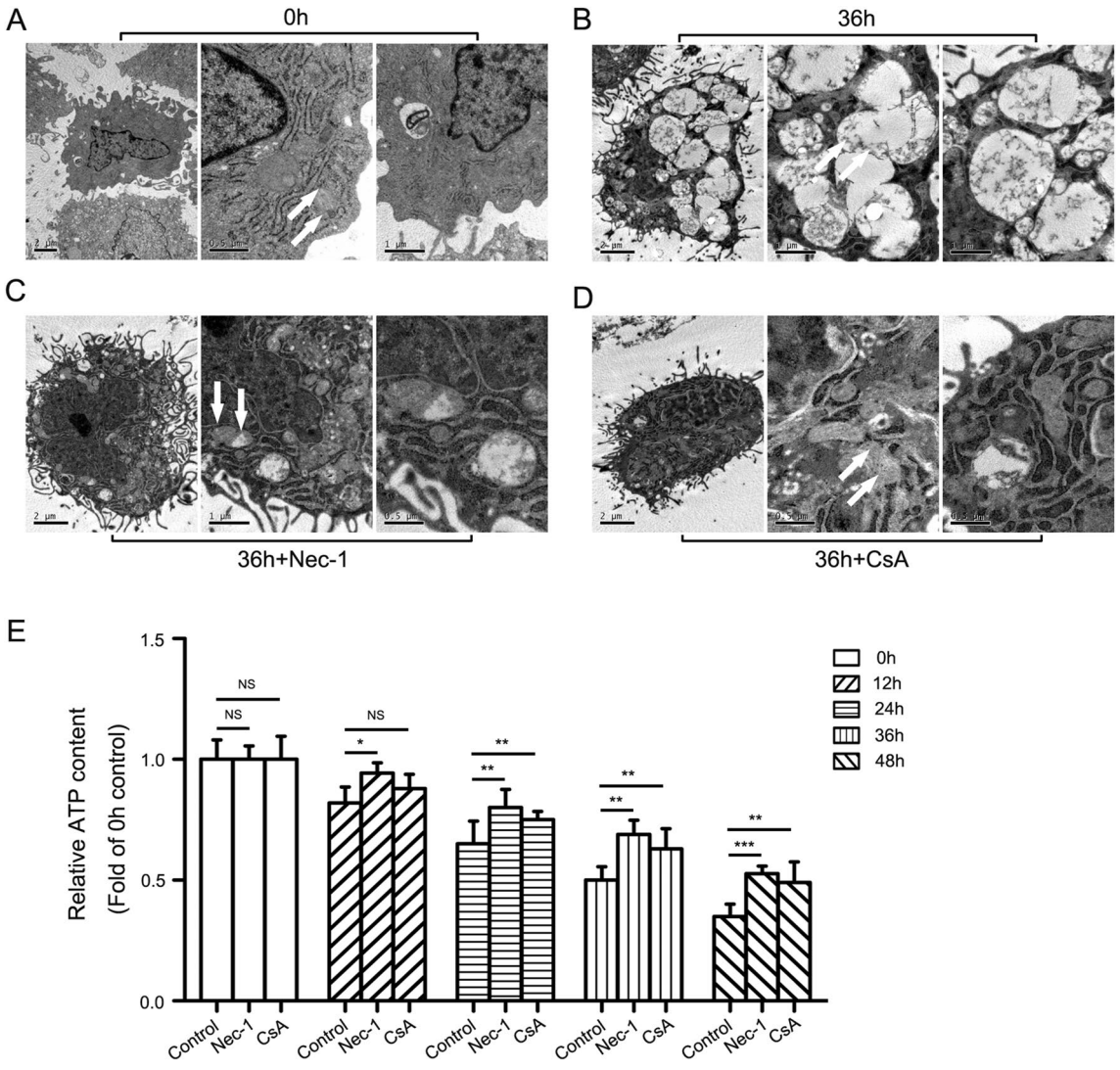

Fig. 2 Nec-1 (20 μM) or CsA (10 μM) ameliorates mitochondrial ultrastructural collapse and ATP depletion induced by compression in rat NP cells. (**a**) (without compression) Displayed normal mitochondria ultrastructure, as the arrowheads indicated. (**b**) (36 h Compression) The arrowheads indicated severe vacuolation and disruption of mitochondria ultrastructure. (**c**–**d**) (36 h Compression + Nec-1 or CsA treated respectively) Nec-1 or CsA could partially reverse the 36 h compression-induced ultrastructural collapse of mitochondrial in NP cells. Scale bars = 2 μM, 1 μM. (**e**) The protective effects of Nec-1 and CsA on rat NP cells ATP depletion using firefly luciferase detection. NS means no significant statistical significance. The values are expressed as mean ± SD from three independent experiments (n = 3, $*P < 0.05$, $**P < 0.01$, $***P < 0.001$ vs. control)

mitochondria from ultrastructural damage in response to compression stimuli.

Nec-1 or CsA blocks ATP depletion induced by compression in NP cells

It was displayed that the production of ATP was decreased in a time-dependent manner and nearly 75% of ATP depleted after 48 h compression in NP cells (Fig. 2e, $P < 0.05$). In presence of Nec-1 (20 μM) or CsA (10 μM), the content of ATP was elevated versus compression without treatment (Fig. 2e, $P < 0.05$). Mitochondria is considered as power factory of the cell, which supply energy required for cell life. Hence, these results indirectly proved that compression led to mitochondrial dysfunction which was obviously improved by Nec-1 or CsA.

Nec-1 or CsA reduces compression-induced oxidative stress in NP cells

Compared to 0 h, ROS production (as indicated by DCHF-DA) was increased at 24 and 36 h of compression (Fig. 3a, b, $P < 0.05$). Then, the content of mtROS was monitored by fluorescent probe MitoSOX. Likewise, an increasing fluorescence intensity of mtROS was observed in 24 and 36 h versus the 0 h (control) group (Fig. 3c, $P < 0.05$). Treatment with Nec-1 (20 μM) or CsA (10 μM) reduced the total ROS and mtROS signals (Fig. 3a–c, $P < 0.05$). Corresponding to these results, the MDA content was markedly increased while a downward trend of SOD activity was observed in NP cells after 24 and 36 h compression (Fig. 3d, e, $P < 0.01$). Treatment with either Nec-1 or CsA attenuated the increase in MDA content and the decrease of SOD activity at both 24 and 36 h time periods (Fig. 3d, e, $P < 0.01$). These results suggested that Nec-1 or CsA might attenuate NP cells necroptosis through attenuating the elevated oxidative stress.

Nec-1, CsA or antioxidant (NAC, BHA) alleviates compression-stimulated NP cells death

The cell viability, lactate dehydrogenase (LDH) release into the culture media from damaged cells (LDH release, indicating cytotoxicity) and PI positive (cell death) ratio were detected to synthetically evaluate the cell survival capacity. Following exposure to compression for 24 and 36 h, 20 μM Nec-1, 10 μM CsA, 5 mM NAC, 200 μM BHA all decreased PI positive ratio and LDH release in NP cells (Fig. 3f–h, $P < 0.05$). Likewise, Nec-1, CsA, NAC, BHA all enhanced NP cell viability at both 24 and 36 h time periods (Fig. 3i, $P < 0.05$). Taken together, these results revealed that Nec-1, CsA and antioxidants exerted a protective effect against compression-induced necroptosis, at least partly, via anti-oxidative stress injury.

RIPK1 is an upstream mediator of compression-induced mitochondrial dysfunction and oxidative stress of NP cells

In this study, when compression was treated for 24 and 36 h, treatment with 20 μM Nec-1 down-regulated RIPK1 expression and activation (pRIPK1), while NAC (5 mM) or BHA (200 μM) had little effects, implying that RIPK1 might be an upstream mediator of oxidative stress (Fig. 4a–d, $P < 0.01$). Considering that Nec-1 efficiently ameliorated mitochondrial dysfunction, we speculated that mitochondrial dysfunction and oxidative stress might play pivotal roles in execution of necroptosis downstream of RIPK1 activation.

Similar to the roles of NAC and BHA, CsA (10 μM) had little effects on RIPK1 expression and activation (pRIPK1), suggesting that mPTP opening might be a downstream consequence of RIPK1 activation (Fig. 4e, f, $P > 0.05$). To determine whether CsA could block the up-regulation of CypD, we performed western blot analysis. The protein expression of CypD was markedly increased when compressed for 24 and 36 h compared to 0 h group. As expected, 10 μM CsA significantly prevented the upregulation of CypD protein expression at both 24 and 36 h compression time periods (Fig. 4e, f, $P < 0.01$).

Nec-1 or CsA blocks mitochondrial apoptotic pathway in compression-treated NP cells

To determine whether Nec-1 or CsA protected NP cells from compression-induced apoptosis, we performed AnnexinV-FITC and PI double staining. After 24 and 36 h compression, Annexin-V positive (apoptosis) ratio was obviously increased compared with 0 h (Fig. 5a, b, $P < 0.01$). Treatment with Nec-1 (20 μM) or CsA (10 μM) down-regulated apoptosis at both 24 and 36 h time periods (Fig. 5a, b, $P < 0.01$). Besides, in presence of Nec-1 or CsA, the green fluorescent signal (apoptosis) was partially reduced at both 24 and 36 h (Fig. 5c).

To further verify Nec-1 or CsA-mediated blockade of apoptosis, we also evaluated the formation of Cleaved Capases. Compared to 0 h group, 24 and 36 h compression elicited notable up-regulation of Cleaved-Caspase3, 8, 9 and PARP in protein level (Fig. 5d, e, $P < 0.01$). Meanwhile, 24 and 36 h compression resulted in significant down-regulation of anti-apoptotic molecule Bcl-2 (Fig. 5d, e, $P < 0.01$). Nec-1 or CsA blocked the up-regulation of Cleaved-Caspase3, 8, 9, PARP as well as the down-regulation of Bcl-2 in protein level (Fig. 5d, e, $P < 0.01$). These results implied that Nec-1 and CsA protected rat NP cells from compression-induced apoptosis.

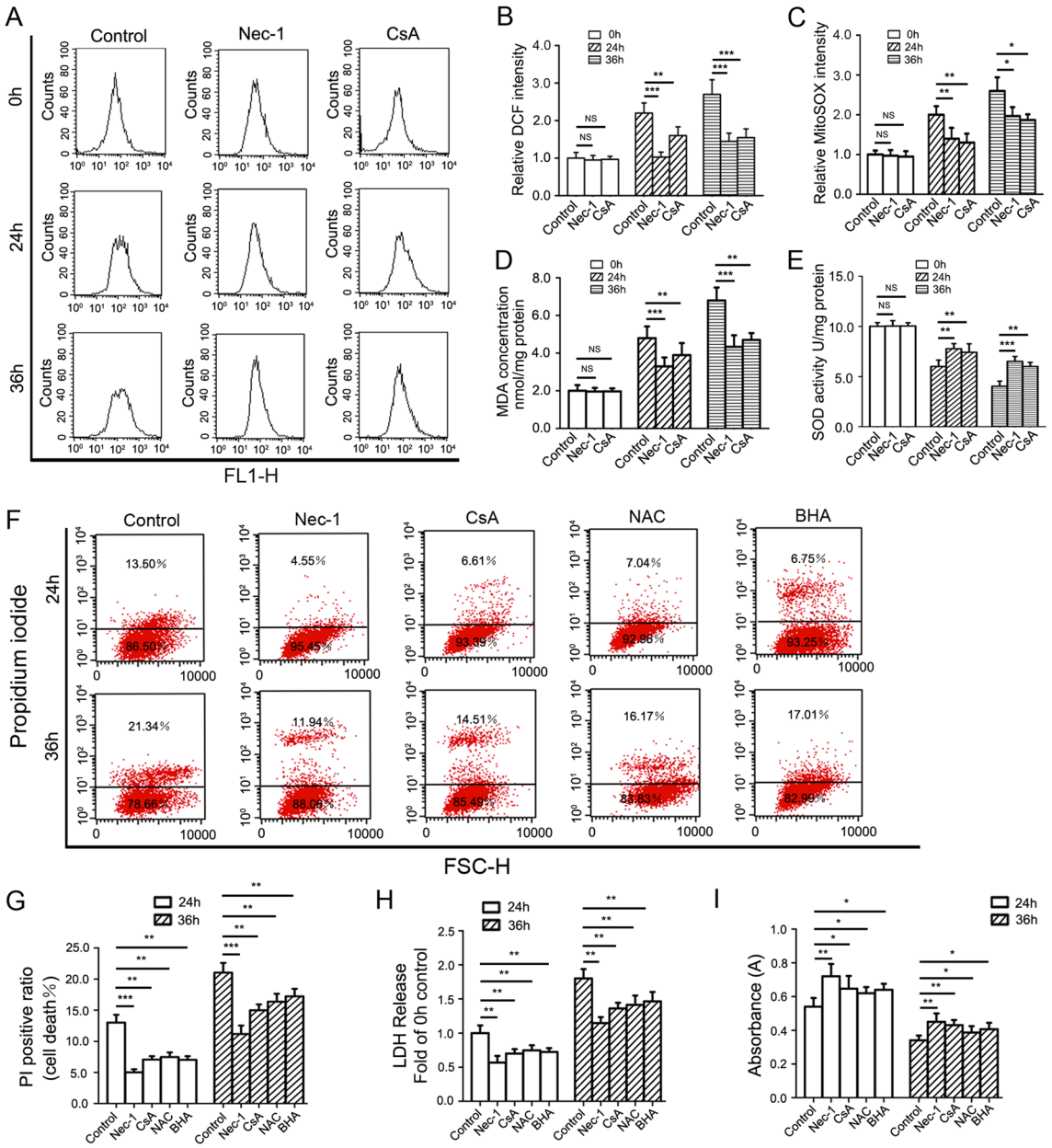

Fig. 3 Nec-1 (20 μM) or CsA (10 μM) alleviates 24 and 36 h compression-induced oxidative stress and cell death in rat NP cells. **a** Representative plots of ROS in NP cells by flow cytometry after the labeling of fluorescent probe DCFH-DA. **b** The quantitative and statistical analysis of ROS generation in NP cells by flow cytometry. **c** The quantitative and statistical analysis of mtROS in NP cells by flow cytometry. **d** The content of MDA was measured with TBA method. **e** The activity of SOD was measured by spectrophotometry. **f**–**g** Representative dot plot (**f**) and statistical analysis (**g**) of PI positive ratio in NP cells by flow cytometry. **h** The cytotoxicity of NP cells was determined by LDH release. **i** The viability of NP cells was measured using the CCK-8 assay. The values are expressed as mean ± SD from four independent experiments (n = 4, $*P < 0.05$, $**P < 0.01$, $***P < 0.001$ vs. control)

Inhibition of apoptosis enhances necroptosis and coordinated regulation of necroptosis and apoptosis promotes NP cells survival more effectively

Then the interplay between necroptosis and apoptosis was explored. As shown in (Fig. 5d, f, $P < 0.01$), the apoptosis inhibitor Z-VAD-FMK (20 μM) treatment downregulated the 24 and 36 h compression induced Cleaved-Caspase3, 8, 9 and PARP expression. However, when treated with Z-VAD-FMK, it was exhibited an enhanced expression of RIPK1 and pRIPK1, suggesting that inhibition of apoptosis might lead to partial conversion to necroptosis (Fig. 5g, $P < 0.01$). Hence, we speculated that the synergistic regulation of

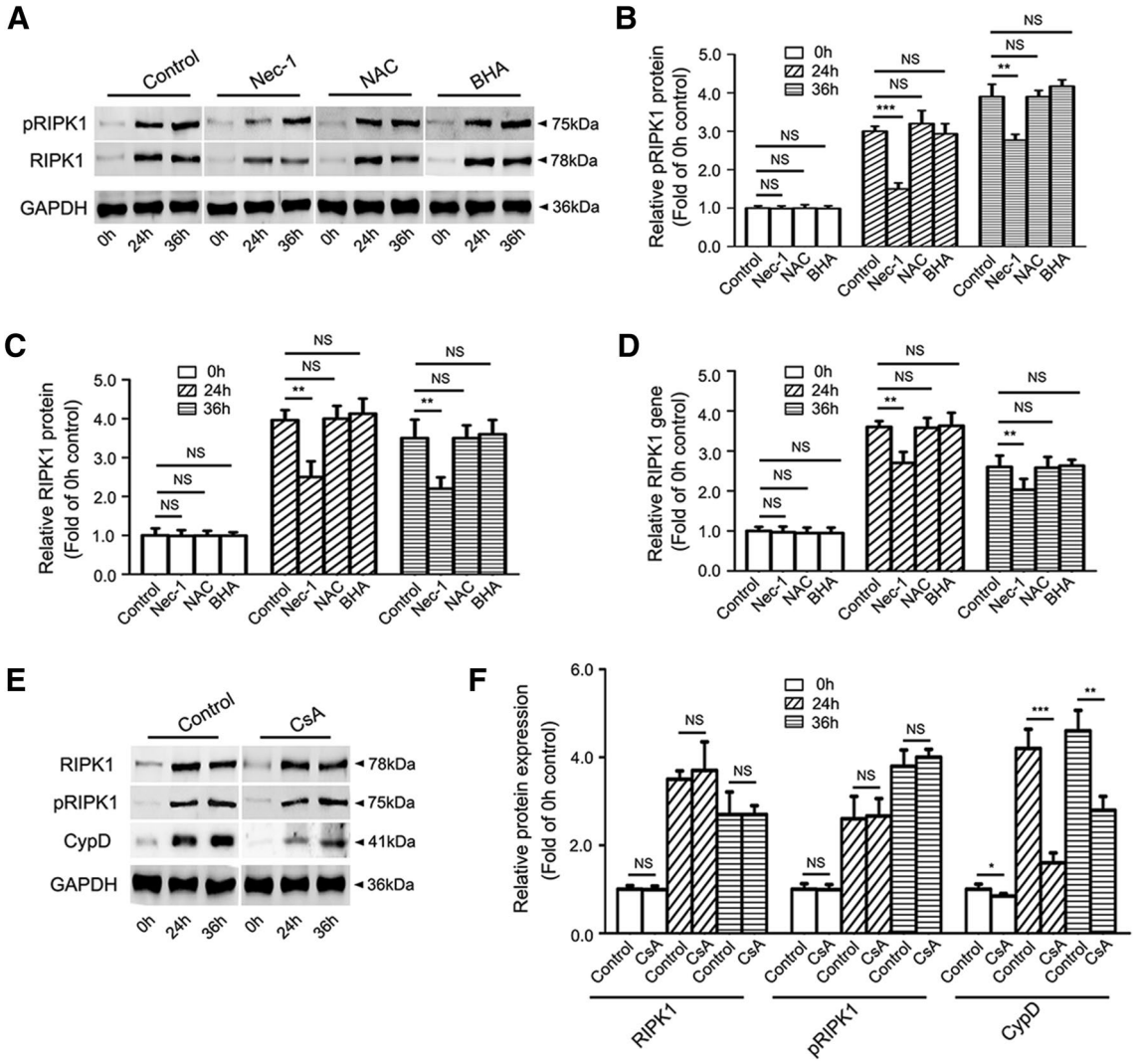

Fig. 4 NAC (5 mM), BHA (200 μM) and CsA (10 μM) have little effects on RIPK1, pRIPK1 expression while CsA down-regulates CypD expression in rat NP cells after 24 and 36 h compression. **a–c** Representative western-blot graphs and statistical analysis of RIPK1, pRIPK1 and GAPDH in NP cells. **d** The mRNA level of RIPK1 was measured by RT-PCR in NP cells. **e–f** Representative western-blot graphs and statistical analysis of RIPK1, pRIPK1, CypD and GAPDH in NP cells. In above, data from treated groups have been normalized to GAPDH. NS means no significant statistical significance. The values are expressed as mean ± SD from three independent experiments (n = 3, $*P < 0.05$, $**P < 0.01$, $***P < 0.001$ vs. control)

necroptosis and apoptosis might be more beneficial in promoting NP cells survival.

In order to verify our hypothesis, the cell viability, LDH release and PI positive ratio assay were performed to thoroughly evaluate the cell death and survival capacity. After 24 and 36 h compression, Nec-1 (20 μM) + Z-VAD-FMK (20 μM) group largely rescued the NP cells viability loss (Fig. 6a, $P < 0.05$). Likewise, Nec-1 + Z-VAD-FMK group also exerted a more effective protective role than Nec-1 or Z-VAD-FMK group alone in reducing PI positive ratio and LDH release (Fig. 6b–d, $P < 0.05$). These results suggested that modulation of necroptosis and apoptosis pathways together was more effective in protecting against compression-induced NP cells death than targeting a specific pathway.

Compression-induced NP cells mitochondrial dysfunction and oxidative stress are not inhibited by SiRIPK1

To interrogate the role of SiRIPK1 in compression-induced NP cells mitochondrial dysfunction and oxidative stress, NP cells were treated with three individual SiRIPK1 sequences. Only one SiRNA sequence 5′-GUC UUCGCUAACACCACUAdTdT-3′, 5′-UAGUGGUGU UAGCGAAGACdTdT-3′ caused a marked decrease

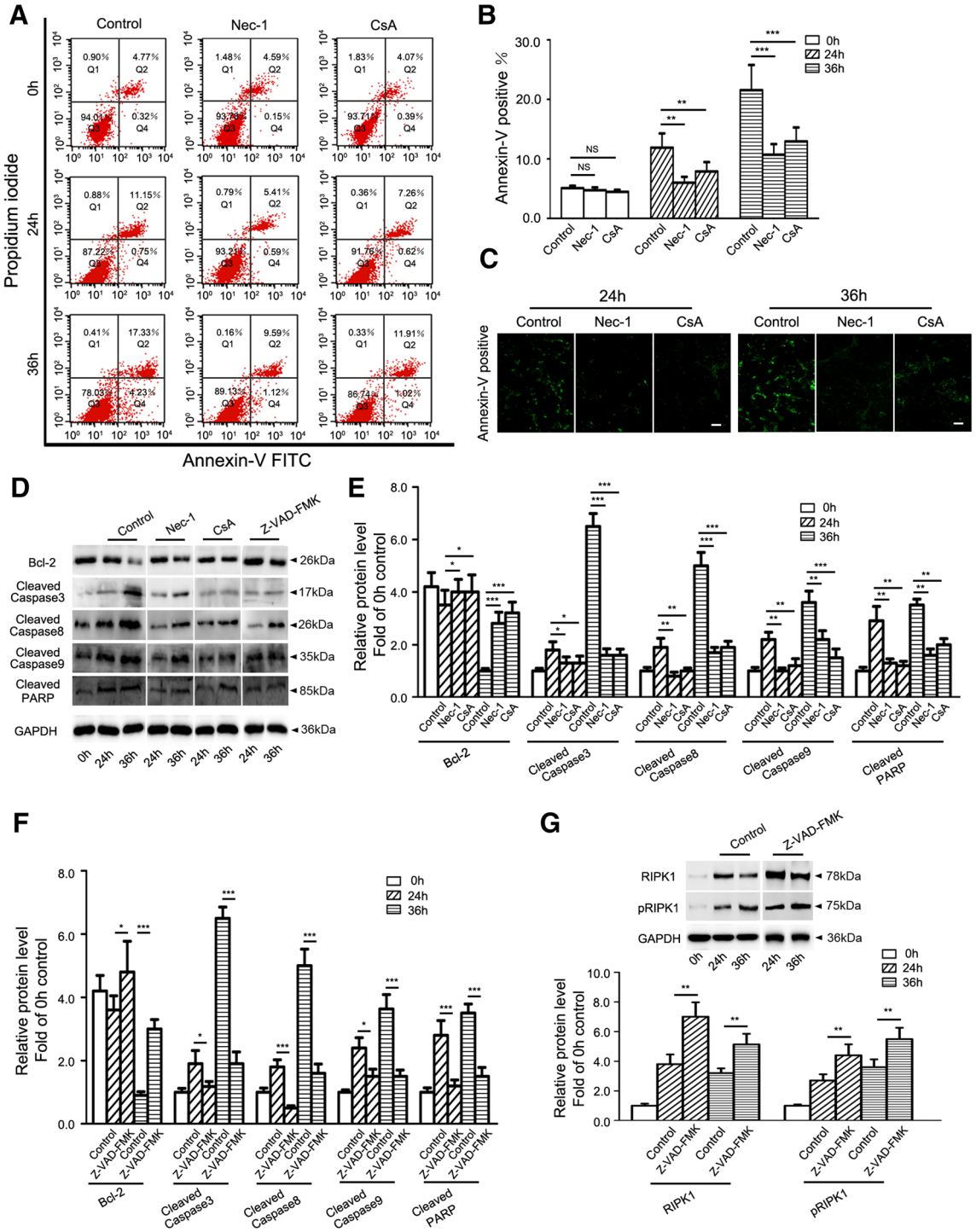

Fig. 5 Nec-1 (20 μM) or CsA (10 μM) attenuates apoptosis while Z-VAD-FMK enhances necroptosis level in rat NP cells after 24 and 36 h compression. **a**–**b** Representative graphs and statistical analysis of apoptosis by flow cytometry after Annexin-V/PI dual staining in NP cells. **c** The fluorescence photomicrograph after Annexin V-FITC staining by LSM in NP cells. **d**–**f** Representative western-blot graphs and statistical analysis of Cleaved-Caspase3, Cleaved-Caspase8, Cleaved-Caspase9, Cleaved-PARP, Bcl-2 and GAPDH in NP cells. **g** Representative western-blot graphs and statistical analysis of RIPK1, pRIPK1 and GAPDH in NP cells. Scale bars = 20 μM. Data from treated groups have been normalized to GAPDH. The values are expressed as mean ± SD from three independent experiments (n = 3, $*P < 0.05$, $**P < 0.01$, $***P < 0.001$ vs. control)

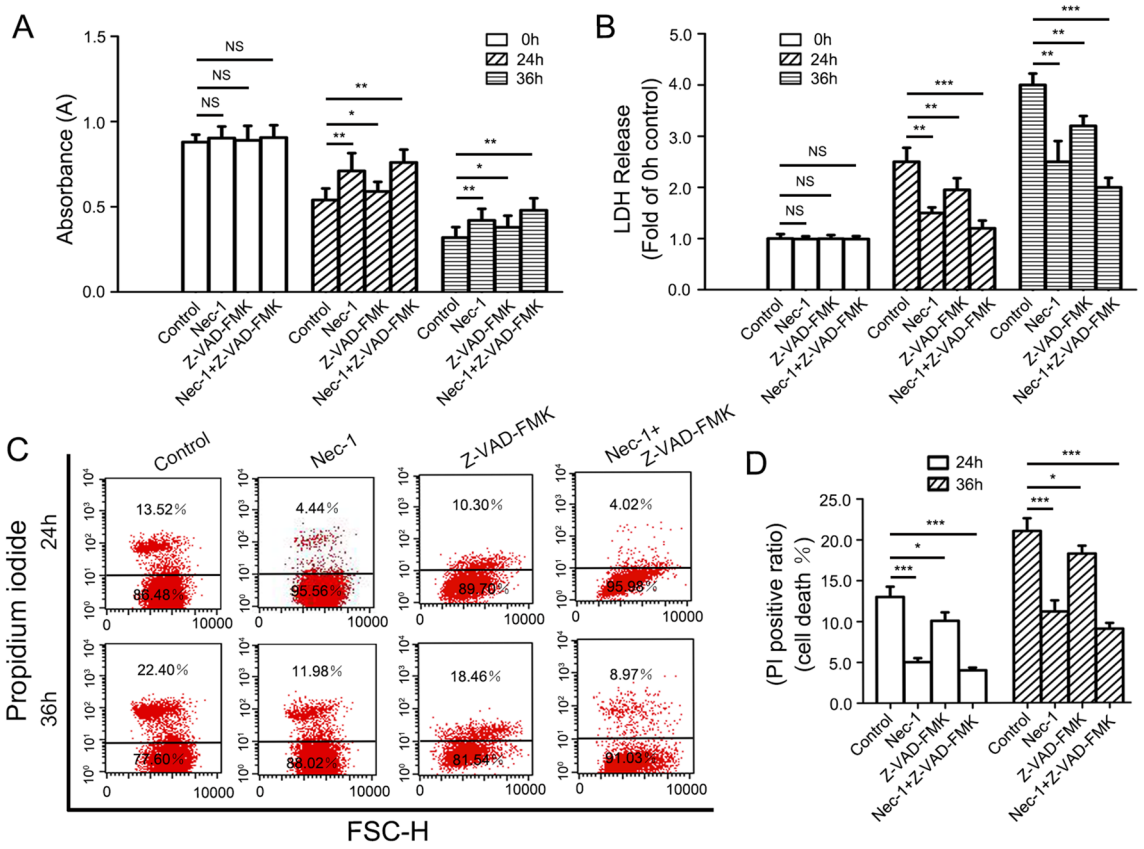

Fig. 6 Combined regulation of necroptosis and apoptosis promotes rat NP cells survival more effectively after 24 and 36 h compression. **a** The viability of NP cells was measured using the CCK-8 assay. **b** The cytotoxicity of NP cells was determined by LDH release. **c** Representative graphs of PI positive ratio by flow cytometry analysis after PI staining in NP cells. **d** The statistical analysis of PI positive ratio in NP cells. The values are expressed as mean ± SD from six independent experiments (n = 6, $*P < 0.05$, $**P < 0.01$, $***P < 0.001$ vs. control)

in protein and gene expression of constitutive RIPK1 (Fig. 7a, $P < 0.001$). The NP cells were treated with this SiRIPK1 for 48 h prior to undergoing 24 and 36 h compression. Contrary to Nec-1 or CsA, SiRIPK1 did not show any protective effect; instead, SiRIPK1 resulted in more severe mitochondrial damage and oxidative stress in NP cells. The SiRIPK1 exhibited greater depolarization of MMP, enhanced mPTP opening and more severe mitochondrial ultrastructural damage compared to untransfected cells (Fig. 7b, c, e, $P < 0.01$). The SiRIPK1 also downregulated the cellular ATP content, which reflected the exacerbated mitochondrial damage (Fig. 7d, $P < 0.01$). Moreover, through ROS detection, MDA content and SOD activity assay, we confirmed that SiRIPK1 exacerbated oxidative stress in NP cells (Fig. 7f–h, $P < 0.05$). Together, contrary to Nec-1, SiRIPK1 triggered more severe mitochondrial dysfunction and oxidative stress in rat NP cells subjected to compression.

Discussion

Mechanical loading is considered as the crucial contributor to IVDD [25, 26]. Researches have demonstrated that a major cause of IVDD is the rate of NP cells death, which is notably increased by compression [6, 27]. In current study, we found for the first time that compression-induced NP cells necroptosis and apoptosis might be tightly relevant to mitochondrial dysfunction-oxidative stress pathway.

As a potential therapeutic target for a variety of diseases, mitochondria are gaining greater attention due to their critical roles in cellular bioenergetics and redox regulation. The specific role of mitochondrial dysfunction in regulating necroptosis and apoptosis remains ambiguous [16, 17]. It was reported that the enhanced mPTP opening led to MMP loss, mitochondrial swelling, vacuolization and even disintegration [28]. Mitochondrial dysfunction is often paralleled

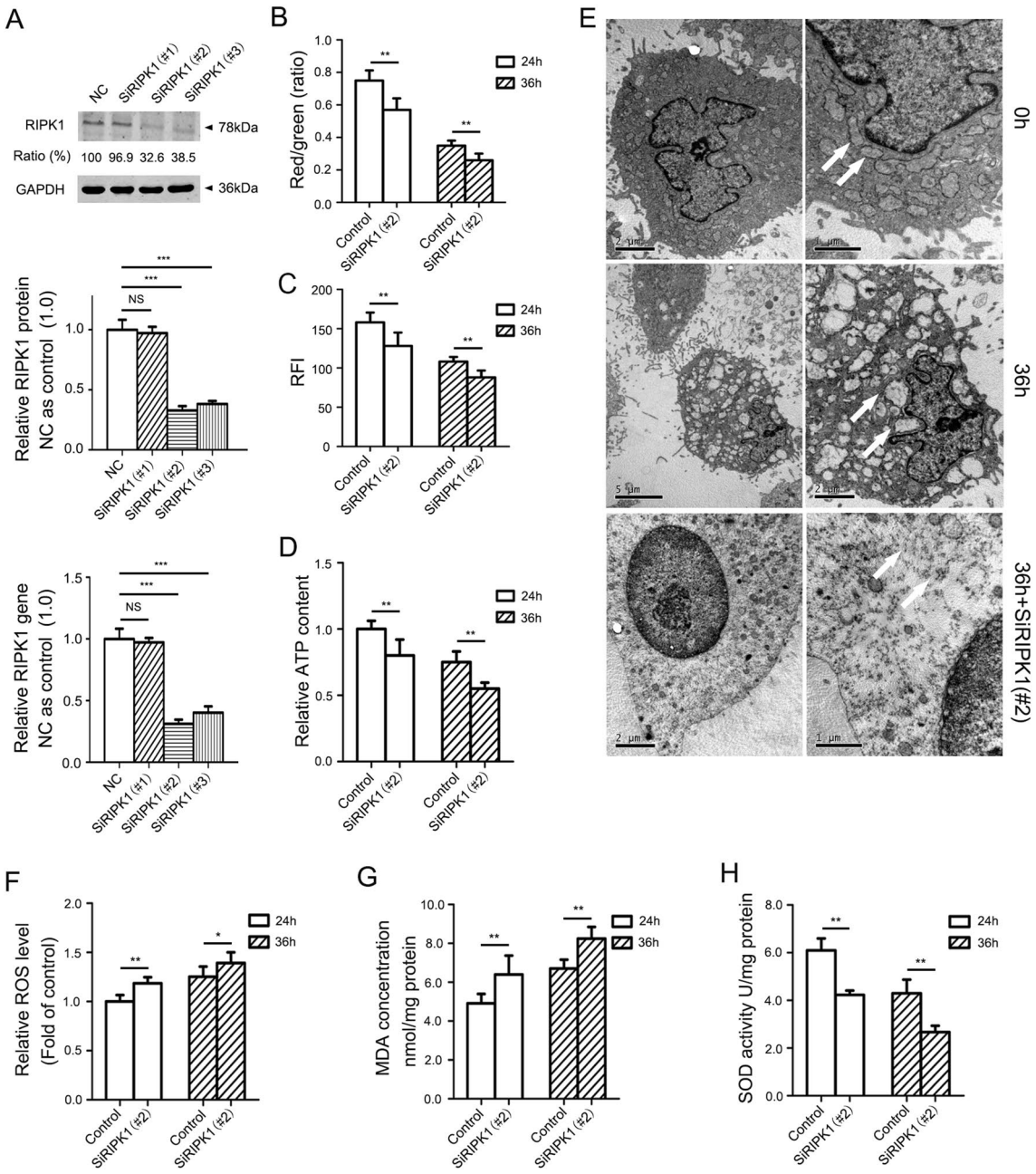

Fig. 7 The SiRIPK1 exacerbates 24 and 36 h compression-mediated mitochondrial damage and oxidative stress in rat NP cells. **a** The NP cells were treated with SiRIPK1 or nonspecific RNA (negative control, NC) for 48 h, then the total protein and gene were measured. The cells were treated with selected SiRIPK1 for 48 h and then compressed for 24 and 36 h. **b–e** The regulative effects of SiRIPK1 on compression-induced MMP loss (**b**), mPTP opening (**c**), ATP depletion (**d**) and mitochondrial ultrastructural damage (**e**) in NP cells. **f–h** The regulative effects of SiRIPK1 on compression-induced ROS generation (**f**), MDA content (**g**) and SOD activity (**h**) in NP cells. Scale bars = 2 μM, 1 μM. The values are expressed as mean ± SD from four independent experiments (n = 4, $*P<0.05$, $**P<0.01$, $***P<0.001$ vs. control)

by elevated oxidative stress, which is combatted by cellular antioxidant systems under normal circumstances. However, oxidative stress is somewhat an enigma in that moderate oxidative stress promotes cell survival, while excessive oxidative stress promotes cell death [19]. Mitochondria are not only a main source of ROS that induce the oxidative stress, but also the vulnerable target of oxidative stress [29]. Mitochondrial damage and oxidative stress may interact with and excite each other, and synergistically regulate the cell death [30]. Likewise, there are some literatures suggesting that mitochondrial dysfunction may act as a crucial role in accelerating IVDD process [31, 32].

In our preliminary experiments, we discovered that compression elicited a time-dependent mPTP opening, MMP loss (depolarization), mitochondrial vacuolation, sharp depletion of ATP and elevation of oxidative stress in NP cells, which directly implied the occurrence of mitochondrial dysfunction. Furthermore, Nec-1 significantly recovered mitochondrial function, confirmed by the observations that Nec-1 notably blocked mPTP opening, MMP loss and mitochondrial ultrastructural collapse. In view of the critical role of mPTP opening, we speculated that the protective effect of Nec-1 might be principally attributed to the restriction of mPTP opening.

The mitochondrial matrix protein CypD is critical structural component of mitochondrial membrane pore. It plays a pivotal role in mPTP opening and subsequently regulates cell proliferation and death [33]. Mice lacking CypD display a greater reduction of infarct size in brain against ischemic injury. Likewise, increased expression of CypD results in greater vulnerability to mPTP in neuronal cells, together with MMP loss following cerebral ischemia in rats [34, 35]. These observation provide the rationale for our treatment with CsA, which interacts with CypD and therefore restricts mPTP opening. Our evidence showed that CsA could exert protective role, and attenuate mitochondrial function damage. CsA mediated blockade of mPTP opening has been considered as a potential target for therapeutic intervention in many kinds of injuries [36, 37]. It remains undetermined whether CsA could block mitochondrial dysfunction and attenuate oxidative stress in rat NP cells induced by compression injury.

Consistent with Nec-1, CsA notably blocked compression-induced mPTP opening and MMP loss. Also, Nec-1 and CsA exerted a high protective effect against mitochondrial ultrastructural collapse and ATP depletion. Given that the enhanced mPTP opening directly leads to mitochondrial damage, the beneficial effects of Nec-1 and CsA may be mediated through reduced mPTP opening. Opening of the mPTP may also be a cause of oxidative stress. The ROS generation and MDA content were obviously elevated after compression treatment. Meanwhile, the SOD activity displayed a notably downward trend. After treatment with Nec-1 or CsA, the ROS generation and MDA content were largely down-regulated while SOD activity was apparently rescued. These suggested that, like Nec-1, CsA might inhibit NP cells necroptosis via minimizing oxidative stress. The protective effects of Nec-1 and CsA on mitochondria might be relevant to the lessening of oxidative stress, thus blocking necroptosis, and improving NP cells survival.

As one important consequence of mitochondrial dysfunction, the ensuing oxidative stress plays a crucial role in a variety of cell death [29]. This finding is further supported by literature showing that the activation of RIPK1 leads to mitochondrial damage, promoting a high level of oxidative stress, and causing cell death [38]. However, the contribution of RIPK1 to oxidative stress remains unknown in compression-treated NP cells. In this study, it was revealed that treatment with CsA or antioxidants (NAC, BHA) had little influence on RIPK1 expression and its phosphorylation. Considering that Nec-1 markedly blocked oxidative stress as above described, we concluded that compression-induced necroptosis may be tightly associated with oxidative stress, which might be induced downstream of RIPK1 activation.

In general, the enhanced mPTP opening exerts a key role in the occurrence of apoptosis. As for the effects of CsA in regulating apoptosis, there exist different views presently. A number of literatures report that CsA significantly block apoptosis, while some other studies display that CsA has little effects on apoptosis [39, 40]. In apoptosis pathway, Cleaved-3, 8, 9 and Cleaved-PARP are important terminal cleavage enzymes. The expression level of Cleaved-3, 8, 9 and Cleaved-PARP were markedly increased after 24 and 36 h compression. Meanwhile, the elevated expression of Cleaved-3, 8, 9 and Cleaved-PARP were all partially attenuated by CsA. The compression elicited a notably decreased in anti-apoptotic key molecule Bcl-2 expression, which was also partially blocked by CsA. Collectively, CsA could efficiently inhibit apoptosis in NP cells. It has been reported that CypD-mediated mPTP opening directly leads to apoptosis [28]. Consistent with mPTP opening, the CypD expression was gradually increased with the extension of compression time, which was inhibited by CsA to some extent. Taken together, these suggested that CypD-mediated mPTP opening might contribute to not only necroptosis but also apoptosis in rat NP cells under compression condition.

Apoptosis is considered a well-defined form of PCD, whereas necroptosis is a novel type of PCD. Under certain circumstance, the cells undergoing necroptosis display activation of apoptotic pathways, yet terminate in a necrosis-like cell death [11]. Necroptosis and apoptosis often interact with each other and synergistically regulate the cell death; however, the precise mechanism remains elusive [11, 23]. Accordingly, the interactive relationship between necroptosis and apoptosis was investigated. It was displayed that Z-VAD-FMK increased RIPK1 and pRIPK1 expression, accompanied with the aggravated mitochondrial dysfunction and elevated oxidative stress, suggesting that apoptosis pathways might be partially progressed toward necroptosis when apoptosis was inhibited. Through detecting and reviewing the key protein of apoptotic pathway such as Cleaved-3, 8, 9, Cleaved-PARP and anti-apopotic protein Bcl-2 together with AnnexinV-FITC positive ratio, we found that Nec-1 efficiently inhibited apoptosis in NP cells. Meanwhile, the combined use of Nec-1 and Z-VAD-FMK (Nec-1 + Z-VAD-FMK) exhibited a more effective role than Nec-1 or Z-VAD-FMK alone in ameliorating NP cells death. Also, Nec-1 + Z-VAD-FMK

largely rescued NP cells viability loss relative to Nec-1 or Z-VAD-FMK alone. These results established that Nec-1 + Z-VAD-FMK acted a more efficient role in protecting against compression-induced NP cells death.

Previously, we confirmed that SiRIPK1 led to significant viability loss and high death rate in NP cells [13]. In this study, SiRIPK1 triggered an exacerbated mitochondrial dysfunction and oxidative stress. In other words, the enhanced expression of RIPK1 may aggravate mitochondrial damage and imbalance of redox reaction; meanwhile, the knockdown of RIPK1 underwent more severe mitochondrial dysfunction and oxidative stress too. Given that the RIPK1 activation can lead to two different outcomes: activation of the NF-κB signaling pathway to promote cell survival, or induction of necroptosis, which leads to cell death [41, 42]. Based on these observations, we speculated that SiRIPK1-induced the exacerbated mitochondrial dysfunction and oxidative stress might be partially due to SiRIPK1 mediated excessive viability loss of NF-κB. In addition, it was confirmed that RIPK1 was essential for activation of mitogen-activated protein kinase (MAPK) and apoptosis [43, 44]. Hence, the exacerbated mitochondrial dysfunction and oxidative stress might also be closely dependent on SiRIPK1-mediated imbalance activation of MAPK and apoptosis. That is to say, the underlying mechanism might be a synergistic regulation of multiple factors, quite complicated process. This will be investigated in detail in our future studies.

In conclusion, this study provides the first evidence that RIPK1-mediated mitochondrial dysfunction and oxidative stress act as a crucial role in NP cells necroptosis and apoptosis under compression-induced injury. CsA-mediated CypD inhibition may provide a new therapeutic platform in protecting NP cells from compression-induced death. We also observed that the synergetic regulation of necroptosis and apoptosis promotes NP cells survival more effectively than that blocking either pathway in isolation. These findings introduce a new perspective to IVDD, and it is extremely expected to offer a more efficient strategy of delaying or even retarding IVDD.

Acknowledgements This study was supported by National Natural Science Foundation of China (Grant No. 81572203), the National Key Research and Development Program of China (Grant No. 2016YFC1100100) and the Youth Innovation Fund of The First Affiliated Hospital of Zhengzhou University (Grant No. YNQN 2017037).

Authors' contribution SC, XL, BH and ZS designed the research. SC, XL, BH and LZ performed the experiments. SC, XL, and SL acquired and analyzed the data. SC, XL, BH, XQ, HL and JX contributed to writing of the manuscript. Finally, all authors have reviewed and approved the final submitted manuscript. The integrity of this work is guaranteed by Dr Songfeng Chen, Dr Xiao Lv, Dr Binwu Hu, and Dr Zengwu Shao.

Compliance with ethical standards

Conflict of interest The authors declare that they have no conflict of interest.

References

1. Yurube T, Hirata H, Kakutani K, Maeno K, Takada T, Zhang Z, Takayama K, Matsushita T, Kuroda R, Kurosaka M, Nishida K (2014) Notochordal cell disappearance and modes of apoptotic cell death in a rat tail static compression-induced disc degeneration model. Arthritis Res Ther 16:R31
2. Yurube T, Takada T, Suzuki T, Kakutani K, Maeno K, Doita M, Kurosaka M, Nishida K (2012) Rat tail static compression model mimics extracellular matrix metabolic imbalances of matrix metalloproteinases, aggrecanases, and tissue inhibitors of metalloproteinases in intervertebral disc degeneration. Arthritis Res Ther 14:R51
3. Sowa G, Agarwal S (2008) Cyclic tensile stress exerts a protective effect on intervertebral disc cells. Am J Phys Med Rehabil 87:537–544
4. Wang C, Gonzales S, Levene H, Gu W, Huang CY (2013) Energy metabolism of intervertebral disc under mechanical loading. J Orthop Res 31:1733–1738
5. Hirata H, Yurube T, Kakutani K, Maeno K, Takada T, Yamamoto J, Kurakawa T, Akisue T, Kuroda R, Kurosaka M, Nishida K (2014) A rat tail temporary static compression model reproduces different stages of intervertebral disc degeneration with decreased notochordal cell phenotype. J Orthop Res 32:455–463
6. Boos N, Weissbach S, Rohrbach H, Weiler C, Spratt KF, Nerlich AG (2002) Classification of age-related changes in lumbar intervertebral discs: 2002 Volvo Award in basic science. Spine J 27:2631–2644
7. Sudo H, Minami A (2011) Caspase 3 as a therapeutic target for regulation of intervertebral disc degeneration in rabbits. Arthritis Rheumatol 63:1648–1657
8. Sudo H, Minami A (2010) Regulation of apoptosis in nucleus pulposus cells by optimized exogenous Bcl-2 overexpression. J Orthop Res 28:1608–1613
9. Ma KG, Shao ZW, Yang SH, Wang J, Wang BC, Xiong LM, Wu Q, Chen SF (2013) Autophagy is activated in compression-induced cell degeneration and is mediated by reactive oxygen species in nucleus pulposus cells exposed to compression. Osteoarthr Cartil 21:2030–2038
10. Degterev A, Huang Z, Boyce M, Li Y, Jagtap P, Mizushima N, Cuny GD, Mitchison TJ, Moskowitz MA, Yuan J (2005) Chemical inhibitor of nonapoptotic cell death with therapeutic potential for ischemic brain injury. Nat Chem Biol 1:112–119
11. Vandenabeele P, Galluzzi L, Vanden Berghe T, Kroemer G (2010) Molecular mechanisms of necroptosis: an ordered cellular explosion. Nat Rev Mol Cell Biol 11:700–714
12. Moriwaki K, Bertin J, Gough PJ, Orlowski GM, Chan FK (2015) Differential roles of RIPK1 and RIPK3 in TNF induced necroptosis and chemotherapeutic agent-induced cell death. Cell Death Dis 6:e1636
13. Chen S, Lv X, Hu B, Shao Z, Wang B, Ma K, Lin H, Cui M (2017) RIPK1/RIPK3/MLKL-mediated necroptosis contributes to compression-induced rat nucleus pulposus cells death. Apoptosis 22:626–638
14. Agarwal S, Yadav A, Tiwari SK, Seth B, Chauhan LK, Khare P, Ray RS, Chaturvedi RK (2016) Dynamin related protein 1 inhibition mitigates bisphenol A-mediated alterations in mitochondrial

dynamics and neural stem cell proliferation and differentiation. J Biol Chem 291:15923–15939
15. Zhou H, Zhu P, Guo J, Hu N, Wang S, Li D, Hu S, Ren J, Cao F, Chen Y (2017) Ripk3 induces mitochondrial apoptosis via inhibition of FUNDC1 mitophagy in cardiac IR injury. Redox Biol 13:498–507
16. Tait SW, Oberst A, Quarato G, Milasta S, Haller M, Wang R, Karvela M, Ichim G, Yatim N, Albert ML, Kidd G, Wakefield R, Frase S, Krautwald S, Linkermann A, Green DR (2013) Widespread mitochondrial depletion via mitophagy does not compromise necroptosis. Cell Rep 5:878–885
17. Moriwaki K, Farias Luz N, Balaji S, De Rosa MJ, O'Donnell CL, Gough PJ, Bertin J, Welsh RM, Chan FK (2016) The mitochondrial phosphatase PGAM5 is dispensable for necroptosis but promotes inflammasome activation in macrophages. J Immunol 196:407–415
18. Liu X, Gao RW, Li M, Si CF, He YP, Wang M, Yang Y, Zheng QY, Wang CY (2016) The ROS derived mitochondrial respiration not from NADPH oxidase plays key role in celastrol against angiotensin II-mediated HepG2 cell proliferation. Apoptosis 21:1315–1326
19. Vanden Berghe T, Vanlangenakker N, Parthoens E, Deckers W, Devos M, Festjens N, Guerin CJ, Brunk UT, Declercq W, Vandenabeele P (2016) Necroptosis, necrosis and secondary necrosis converge on similar cellular disintegration features. Cell Death Differ 17:922–930
20. Jiang YQ, Chang GL, Wang Y, Zhang DY, Cao L, Liu J (2016) Geniposide prevents hypoxia reoxygenation-induced apoptosis in H9c2 cells: improvement of mitochondrial dysfunction and activation of GLP-1R and the PI3K/AKT signaling pathway. Cell Physiol Biochem 39:407–421
21. Ahsan A, Han G, Pan J, Liu S, Padhiar AA, Chu P, Sun Z, Zhang Z, Sun B, Wu J, Irshad A, Lin Y, Peng J, Tang Z (2015) Phosphocreatine protects endothelial cells from oxidized low-density lipoprotein-induced apoptosis by modulating the PI3K/Akt/eNOS pathway. Apoptosis 20:1563–1576
22. Ding F, Shao ZW, Yang SH, Wu Q, Gao F, Xiong LM (2012) Role of mitochondrial pathway in compression-induced apoptosis of nucleus pulposus cells. Apoptosis 17:579–590
23. Seya T, Shime H, Takaki H, Azuma M, Oshiumi H, Matsumoto M (2012) TLR3/TICAM-1 signaling in tumor cell RIP3-dependent necroptosis. Oncoimmunology 1:917–923
24. Zhao L, Lin H, Chen S, Chen S, Cui M, Shi D, Wang B, Ma K, Shao Z (2017) Hydrogen peroxide induces programmed necrosis in rat nucleus pulposus cells through the RIP1/RIP3-PARP-AIF pathway. J Orthop Res. https://doi.org/10.1002/jor.23751
25. Wang F, Cai F, Shi R, Wang XH, Wu XT (2016) Aging and age related stresses: a senescence mechanism of intervertebral disc degeneration. Osteoarthr Cartil 24:398–408
26. Jiang LB, Cao L, Yin XF, Yasen M, Yishake M, Dong J, Li XL (2015) Activation of autophagy via Ca^{2+} dependent AMPK/mTOR pathway in rat notochordal cells is a cellular adaptation under hyperosmotic stress. Cell Cycle 14:867–879
27. Hunter CJ, Matyas JR, Duncan NA (2003) The notochordal cell in the nucleus pulposus: a review in the context of tissue engineering. Tissue Eng 9:667–677
28. Liu G, Wang ZK, Wang ZY, Yang DB, Liu ZP, Wang L (2016) Mitochondrial permeability transition and its regulatory components are implicated in apoptosis of primary cultures of rat proximal tubular cells exposed to lead. Arch Toxicol 90:1193–1209
29. Carlisi D, Buttitta G, Di Fiore R, Scerri C, Drago-Ferrante R, Vento R, Tesoriere G (2016) Parthenolide and DMAPT exert cytotoxic effects on breast cancer stem-like cells by inducing oxidative stress, mitochondrial dysfunction and necrosis. Cell Death Dis 7:e2194
30. Chen Q, Chen X, Han C, Wang Y, Huang T, Du Y, Dong Z (2016) FGF-2 transcriptionally down-regulates the expression of BNIP3L via PI3K/Akt/FoxO3a signaling and inhibits necrosis and mitochondrial dysfunction induced by high concentrations of hydrogen peroxide in H9c2 cells. Cell Physiol Biochem 40:1678–1691
31. Xu D, Jin H, Wen J, Chen J, Chen D, Cai N, Wang Y, Wang J, Chen Y, Zhang X, Wang X (2017) Hydrogen sulfide protects against endoplasmic reticulum stress and mitochondrial injury in nucleus pulposus cells and ameliorates intervertebral disc degeneration. Pharmacol Res 117:357–369
32. Niu CC, Lin SS, Yuan LJ, Chen LH, Wang IC, Tsai TT, Lai PL, Chen WJ (2013) Hyperbaric oxygen treatment suppresses MAPK signaling and mitochondrial apoptotic pathway in degenerated human intervertebral disc cells. J Orthop Res 31:204–209
33. Itani HA, Dikalova AE, McMaster WG, Nazarewicz RR, Bikineyeva AT, Harrison DG, Dikalov SI (2016) Mitochondrial cyclophilin D in vascular oxidative stress and hypertension. Hypertension 67:1218–1227
34. Abramov AY, Duchen MR (2008) Mechanisms underlying the loss of mitochondrial membrane potential in glutamate excitotoxicity. Biochim Biophys Acta 1777:953–964
35. Fakharnia F, Khodagholi F, Dargahi L, Ahmadiani A (2017) Prevention of cyclophilin D-mediated mPTP opening using cyclosporine-A alleviates the elevation of necroptosis, autophagy and apoptosis-related markers following global cerebral ischemia-reperfusion. J Mol Neurosci 61:52–60
36. Li S, Guo J, Ying Z, Chen S, Yang L, Chen K, Long Q, Qin D, Pei D, Liu X (2016) Valproic acid-induced hepatotoxicity in Alpers syndrome is associated with mitochondrial permeability transition pore opening-dependent apoptotic sensitivity in an induced pluripotent stem cell model. Hepatology 61:1730–1739
37. Gharanei M, Hussain A, Janneh O, Maddock HL (2013) Doxorubicin induced myocardial injury is exacerbated following ischaemic stress via opening of the mitochondrial permeability transition pore. Toxicol Appl Pharmacol 268:149–156
38. Ye YC, Wang HJ, Yu L, Tashiro S, Onodera S, Ikejima T (2012) RIP1-mediated mitochondrial dysfunction and ROS production contributed to tumor necrosis factor alpha-induced L929 cell necroptosis and autophagy. Int Immunopharmacol 14:674–682
39. Kim SY, Shim MS, Kim KY, Weinreb RN, Wheeler LA, Ju WK (2014) Inhibition of cyclophilin D by cyclosporin A promotes retinal ganglion cell survival by preventing mitochondrial alteration in ischemic injury. Cell Death Dis 5:e1105
40. Zhu XD, Chi JY, Liang HH, Huangfu LT, Guo ZD, Zou H, Yin XH (2016) MicroRNA-377 mediates cardiomyocyte apoptosis induced by cyclosporin A. Can J Cardiol 32:1249–1259
41. Geng J, Ito Y, Shi L, Amin P, Chu J, Ouchida AT, Mookhtiar AK, Zhao H, Xu D, Shan B, Najafov A, Gao G, Akira S, Yuan J (2017) Regulation of RIPK1 activation by TAK1-mediated phosphorylation dictates apoptosis and necroptosis. Nat Commun 8:359
42. Christofferson. Dana E, Yuan. Junying (2010) Necroptosis as an alternative form of programmed cell death. Curr Opin Cell Biol 22:263–268
43. Kelliher MA, Grimm S, Ishida Y, Kuo F, Stanger BZ, Leder P (1998) The death domain kinase RIP mediates the TNF-induced NF-kappaB signal. Immunity 8:297–303
44. Obitsu S, Sakata K, Teshima R, Kondo K (2013) Eleostearic acid induces RIP1-mediated atypical apoptosis in a kinase-independent manner via ERK phosphorylation, ROS generation and mitochondrial dysfunction. Cell Death Dis 4:e674